

Research Article

Abduldaem S. Alqasemi, Majed Ibrahim*, Ayad M. Fadhil Al-Quraishi, Hakim Saibi, A'kif Al-Fugara, and Gordana Kaplan

Detection and modeling of soil salinity variations in arid lands using remote sensing data

<https://doi.org/10.1515/geo-2020-0244>

received September 26, 2020; accepted March 15, 2021

Abstract: Soil salinization is a ubiquitous global problem. The literature supports the integration of remote sensing (RS) techniques and field measurements as effective methods for developing soil salinity prediction models. The objectives of this study were to (i) estimate the level of soil salinity in Abu Dhabi using spectral indices and field measurements and (ii) develop a model for detecting and mapping soil salinity variations in the study area using RS data. We integrated Landsat 8 data with the electrical conductivity measurements of soil samples taken from the study area. Statistical analysis of the integrated data showed that the normalized difference vegetation index and bare soil index showed moderate correlations among the examined indices. The relation between these two indices can contribute to the development of successful soil salinity prediction models. Results show that 31% of the soil in the study area is moderately saline and 46% of the soil is highly saline. The results support that geoinformatic techniques using RS data and technologies constitute an effective tool for detecting soil salinity by modeling and mapping the spatial distribution of saline soils. Furthermore, we observed a low correlation between soil salinity and the nighttime land surface temperature.

* **Corresponding author: Majed Ibrahim**, Geographic Information System and Remote Sensing Department, Erath and Environmental Science Institute, Al al-Bayt University, Al Mafrqa, Jordan, e-mail: majed.ibrahim@aabu.edu.jo

Abduldaem S. Alqasemi: Geography and Urban Sustainability, College of Humanities & Social Science, UAEU, Al-Ain, United Arab Emirates

Ayad M. Fadhil Al-Quraishi: Surveying and Geomatics Engineering Department, Faculty of Engineering, Tishk International University, Erbil, Iraq

Hakim Saibi: Geology Department, College of Science, UAEU, Al-Ain, United Arab Emirates

A'kif Al-Fugara: Surveying Engineering Department, Engineering-College, Al al-Bayt University, Al Mafrqa, Jordan

Gordana Kaplan: Institute of Earth and Space Sciences, Eskisehir Technical University, Eskisehir, Turkey

Keywords: electrical conductivity, remote sensing, Landsat 8, salinity salinization, spectral index, LST

1 Introduction

Soil salinization, which is a common form of soil degradation, is one of the world's most widespread environmental problems [1–5]. This global problem results in land degradation, especially in irrigated areas in arid and semiarid environments as well as in some subhumid regions [3,6]. Soil salinization has become increasingly serious in recent decades, with salinization exceeding the average level of soil salinity in the past few years because of unsustainable agricultural practices that lead to the accumulation of soluble salts in soil [3,5,7,8]. Soil salinization reduces the land value and productivity [9,10]. By reducing the soil quality, soil salinization limits the suitability of the land for agriculture or reclamation and can increase soil dispersion and erosion.

Soil salinization is a severe environmental hazard that influences almost half of the existing irrigation plans of worldwide soils facing the threat of secondary salinization [3,11,12]. General estimates indicate that approximately 1 billion hectares of land are affected by salinization worldwide, constituting 7% of the continental area of the Earth and 58% of the irrigated land [3,13,14]. The main causes of soil salinization in dry regions include irrigation (i.e., overpumping), poor water drainage, and climate change [15–19]. Therefore, areas of agricultural or arable lands will dwindle because of salinization [5]. Additionally, many countries are confronted with varying degrees of soil salinization. The Food and Agriculture Organization has estimated that 397 million hectares of the world's agricultural or nonagricultural lands have been affected by soil salinization [3,6,10,11,20,21]. Thus, it is crucial to determine which lands are affected by soil salinization, evaluate soil salinity, and determine the root causes of salinization to help decision makers develop management plans for ensuring the sustainability of

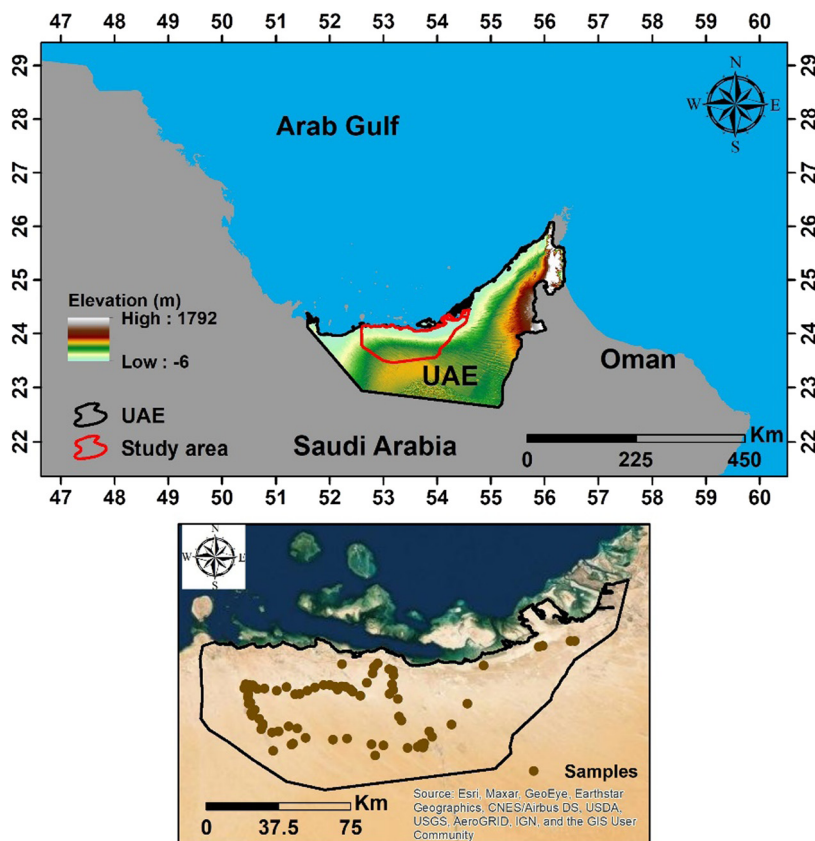


Figure 1: Locations of the study area and sampling sites.

agricultural land. This must be prioritized globally because soil salinization has deleterious impacts on the soil quality and productivity and is ubiquitous in the arid and semiarid parts of the world [1,3,22,23].

Researchers have recently shown significant interest in evaluating and mapping soil salinity in many regions around the world, especially in arid and semiarid areas that are heavily affected by salinization. For soil salinity evaluation and mapping, data must be collected using traditional soil sampling and laboratory analysis methods. However, these methods are time-consuming and costly, thereby limiting surveys to small areas [1,3,5,24]. To overcome this limitation, several techniques have been developed for evaluating soil salinity. One such technique is based on remote sensing (RS), which has demonstrated considerable success in mapping and assessing soil salinity [5,25,26].

Metternicht [27], Metternicht and Zinck [28], Eldeiry and Garcia [29], and Furby *et al.* [30] observed that meaningful results could be obtained by studying the spectral properties and radar backscatter of saline soils. Some

researchers (e.g., ref. [31]) have studied soil salinity based on moisture content using the normalized difference infrared index. Other researchers have assessed the relations between soil salinity and vegetation indices [5,26,32–36]. Other studies have analyzed soil salinity using the thermal and short infrared wavelength bands [3,5,28,34,37] to examine the relation between soil salinity and the land surface temperature (LST). These studies used satellite imagery containing thermal bands such as a moderate resolution imaging spectroradiometer (MODIS), which provides useful information about the soil properties [38–40]. Recently, the multispectral data derived from sources, such as the System Pour I, Observation de la Terre (SPOT), IKONOS, Quick Bird, Indian Remote Sensing, and Landsat satellites, have been used to explore map soil salinity. Several other indices, such as the salinity index [41] and the soil adjusted vegetation index [42], are also commonly employed to monitor soil salinity. However, Eldeiry and Garcia [29] and Hu *et al.* [43] recommended the combined use of spectral response index and best band [44,45].

The RS tools and data must be integrated with the field measurements of salinity to achieve soil salinity evaluation and monitoring. RS is an efficient tool for spatial analysis of soil salinity in arid and semiarid areas; therefore, we aimed to estimate the soil salinity in Abu Dhabi using specific spectral indices combined with field measurements. The soil salinity mapping model developed in this study is based on the electrical conductivity (EC) of soil and shows a promising correlation, which can be further improved by considering the soil salinity–LST relation. This model is helpful to develop effective soil salinity forecasting strategies for sustainable development and land management.

2 Methods

2.1 Study area

The study area is located in the western part of the United Arab Emirates (UAE) near the coast of Abu Dhabi (Figure 1). The study area covers parts of the central and southwestern areas of Abu Dhabi and lies between 24.44° and 23.46°N latitude and 52.59° and 54.49°E longitude.

The study area exhibits a hot arid climate with high temperatures through the night during summer. The mean minimum and maximum summer temperatures are 21.7 and 33°C, respectively [9,46]. In the zones away from the Sabkha area, mean temperatures can reach 43°C in summer and 17°C in winter [47,48]. The mean annual rainfall is slightly less than 120 mm, which corresponds to extremely arid climatic conditions. This rainfall is 37% of the precipitation near the Strait of Hormuz, 40–50% of that in the shallow depths of the UAE coastal areas, 60–70% of that in lagoons and embayments, and 65% of that in the Arabian Gulf coastal lagoons [47,49–52]. Aridisols, Entisols, and Inceptisols types of soil covered Emirate, where the soils have been classified into three soil orders [53]. Most of the Emirate areas were covered by Entisols, then Aridisols to a lesser extent, and Inceptisols are the least common in the region. Entisols and Aridisols are the types of soil that covered Abu Dhabi [54,55].

The study area is categorized as one of the largest Sabkha surfaces, both coastal and inland, in the world. This region is dominated by the hot arid climate zone, as evidenced by the salt flats and marshes, which are categorized as the geological features of Sabkha commonly observed under arid and semiarid climatic conditions [47,51].

Evaporation is considerably higher because of the extremely hot climatic conditions of the study area. This results

in the deposition of large amounts of salts in the soil, increasing the percentage of insoluble salts beyond saturation. These factors and the associated soil salinization pose serious environmental threats to the soil environment in the Sabkha area. Soil degradation leads to decreased soil productivity, and uneven dehydration of gypsum contributes to the development of cracks in the soil surface. High concentrations of sulfate and carbonate salts lead to the corrosion of the steel pipes of water and oil distribution networks [9,56].

3 Methodology

The methods followed in this study can be broadly divided into three categories: (i) field measurements, (ii) image processing, and (iii) statistical analysis.

3.1 *In situ* and laboratory measurements

After consideration of heterogeneity, soil samples of different types of with diverse salinity levels were collected from 80 sites in a desert area with dominant sand dunes. Soil samples were collected in two directions along a stretch of the existing roads in the study area at different distance to ensure that the samples covered different types of land and included inland Sabkha and saline soil areas. The samples were divided into two groups, i.e., soil samples collected from the areas in dune zones near major roads and those collected from the inland Sabkha and saline soil areas. This categorization of the soil samples allowed the assessment of the soil salinity and degradation index. Some samples from both groups were used in salinity estimation and model development, and the remaining samples were employed for model validation. The fieldwork was conducted in November 2016, and sampling was performed during dry weather conditions, indicating the occurrence of no rainfall in the study area during sample collection.

The soil samples were analyzed in the laboratories of United Arab Emirates University. Following the standard soil analysis methods presented by Evans et al. [51], the soil samples were air-dried at room temperature, fragmented by hand or using a geological hammer, and then ground. A 1:2 soil–water suspension was prepared by mixing the soil mass with a volume of deionized water equivalent to double the soil mass. An EC meter (ExStik EC 400) was used to measure the conductance of the

soil suspension to indicate the amount of soluble salts in the soil. This EC meter measures conductivity in the ranges of 0–199.9, 200–1999, and 2.00–19.99 mS/cm. Soil samples with EC values higher than the EC meter's upper limit were further diluted to enable accurate EC measurements.

Following Kissel and Sonon [57], soil salinity was classified into three classes in terms of soil quality and suitability for plant growth, as shown in Table 1. Previous research projects developed soil salinity scales (e.g., the soil quality guideline) in terms of the sodium adsorption ratio and EC for unrestricted land use [7,57]. The comparison of the soil EC values obtained in this study with the soil salinity scale found in the Soil Test Handbook for Georgia [57] indicates that most of the study samples are in the very high salinity level.

3.2 Data acquisition

The RS data for this research were downloaded from the US Geological Survey Earth Explorer (<https://earthexplorer.usgs.gov/>). The data collected were the Landsat 8 Operational Land Imager (OLI) and day and night MODIS LST data (Aqua and Terra) MYD11A1 and MOD11A1, which were geometrically corrected and rectified to UTM zone 39. The images acquired on November 6, 2016 (path 161 and rows 43 and 44) were utilized to correspond with the fieldwork. MODIS data with horizontal (h) and vertical (v) title number h22v06 were downloaded. All image data were prepared and analyzed after performing atmospheric correction. The images were indexed and analyzed and the database created. The GIS environment tools were used to compose the images and to map soil salinity. MODIS/Terra and Aqua satellite imageries were used to examine the correlation between *in situ* salinity measurements and LST values obtained from satellite imagery in the study area. The results were analyzed statistically using Microsoft Excel.

Table 1: Soil salinity classes (modified from Kissel and Sonon [57])

EC (dS/m)	Soil salinity class	Description
<1	Low	– Plants may starve if the soil lacks organic matter – Satisfactory if the soil contains abundant organic matter
1–2	Medium	The satisfactory range for established plants
>2.00	High	– Suitable for some types of plants and unsuitable for seedlings or cuttings – If the EC increases to more than 2 dS/m, then the soil will be unsuitable for plant growth – Plants will be severely dwarfed, and the seedlings and rooted cuttings will frequently die

3.3 Image analysis

Four spectral indices were utilized in this study to achieve the study objectives. These indices are normalized difference vegetation index (NDVI), the bare soil index (BSI), the spectral salinity index 1 (SSI1), and SI.

3.4 NDVI

NDVI represents the normalized ratio of near-infrared and red reflectance has been used in many scientific studies related to environmental issues such as soil and vegetation degradation [58]. NDVI is calculated as follows:

$$\text{NDVI} = \frac{\lambda \text{ NIR} - \lambda \text{ Red}}{\lambda \text{ NIR} + \lambda \text{ Red}}, \quad (1)$$

where NIR is the near-infrared reflectance ($\lambda \approx 0.8 \mu\text{m}$) and red is the red-band reflectance ($\lambda \approx 0.64 \mu\text{m}$). Variations in soil brightness can lead to noticeable variations in NDVI values [59].

3.5 BSI

BSI is the second index considered in this study. It combines the surface reflections of blue, red, green, and near-infrared radiation and is employed to detect soil variations from the Landsat 8 OLI and Thematic Mapper images. BSI was used to assess the condition of barren soil, which is helpful in determining the state of land degradation because of salinity. BSI also helps to determine the relation between soil salinity and plant growth, mainly in the coastal and inland Sabkha that covers most of the study area [60]. BSI is calculated as follows [61]:

$$\text{BSI} = \left[\frac{(\lambda \text{ Red} + \lambda \text{ Green}) - (\lambda \text{ Red} + \lambda \text{ Blue})}{(\lambda \text{ NIR} + \lambda \text{ Green}) + (\lambda \text{ Red} + \lambda \text{ Blue})} \times 100 \right] + 100 \quad (2)$$

3.6 SSI1

SSI1 was also employed in this study. It is one of the common indices used to estimate soil salinity in dry land and in arid and semiarid areas, and it is sensitive to the soil salinity in arid and semiarid regions [60]. SSI1 is calculated as follows [60]:

$$\text{SSI1} = \sqrt{\text{Blue}} \times \text{SWIR2}, \quad (3)$$

where SWIR2 is the shortwave infrared-2 reflectance ($\lambda \approx 2.2 \mu\text{m}$) and blue is the blue-band reflectance ($\lambda \approx 0.48 \mu\text{m}$).

3.7 SI

SI is the salinity index derived from the broadband satellite images that indicate the relation between the actual soil salinity and the variation in vegetation. Thus, many studies have evaluated soil salinity by referring to vegetation reflectance [62]. This index is defined as the square root of the reflectance of blue radiation multiplied by the reflectance of the red radiation [63].

$$\text{SI} = \sqrt{\text{Blue}} \times \text{Red}, \quad (4)$$

where blue and red denote the reflectance in the blue and red light regions of the spectrum ($\lambda \approx 0.48 \mu\text{m}$ and $\lambda \approx 0.64 \mu\text{m}$), respectively.

3.8 LST

Temperature was converted from kelvin (K) to Celsius ($^{\circ}\text{C}$) using the following equation. First, we multiplied the unit by an assigned scale factor of 0.02 to obtain the value in kelvin, after which the resulting value was subtracted by 273.15 to convert K to $^{\circ}\text{C}$.

$$\text{LST} (^{\circ}\text{C}) = a \times \text{DN} - 273.15 \quad (5)$$

where $^{\circ}\text{C}$ is the LST in Celsius and a is the scaling factor of the MODIS LST product [43].

4 Results and discussion

Results of the laboratory analyses of soil samples indicated that although nonsaline soils characterize certain parts of the study area, soils in the majority of the Sabkha

Table 2: Descriptive statistics for five study variables (EC, SI, SSI1, NDVI, and BSI)

Parameter	EC (dS/m)	SI	SSI1	NDVI	BSI
Min.	0.09	0.06	0.10	0.00	0.6
Max.	170.10	0.18	0.26	0.10	0.12
Mean	15.67	0.08	0.21	0.07	0.08
Standard deviation	32.66	0.03	0.03	0.02	0.03
Standard error	3.65	0.00	0.00	0.00	0.00

Table 3: Results of the analysis of correlation among the study variables

Variable	Soil salinity	SI	SSI1	BSI	NDVI
Soil salinity	1				
SI	0.21	1			
SSI1	0.21	0.26	1		
BSI	0.25	0.23	0.41	1	
NDVI	0.43	0.19	0.46	0.80	1

Note: The significance for all bold values were less than 0.05.

area are highly saline (Table 3). The highly saline parts of Sabkha area are categorized as salt flats. Additionally, although the maximum EC value in the study area is 170.1 dS/m, most of the nonsaline soil locations are located far from the Sabkha and have a minimum EC value of 0.09 dS/m. Statistical analyses were conducted on the five main study variables: EC, SI, SSI1, NDVI, and BSI (Table 2).

NDVI and BSI show the strongest correlations with soil salinity, with coefficient of determination (R^2) values of 0.43 and 0.25, respectively (Table 3). Regression analysis demonstrates that the model predicting EC from NDVI and BSI has a prediction power of 80%, as indicated by an R^2 value of 0.80. Thus, only NDVI and BSI were used to generate the final salinity model for the study area. Results reveal that the probability (p) values were less than 0.05, indicating a statistically significant correlation between the RS data and field measurements. Thus, these data can be used to model the spatial distribution of soil salinity in the study area.

4.1 Relation between vegetation indices and soil salinity

The soil analysis results show that the relation between NDVI and soil salinity is statistically significant ($R^2 = 0.43$, $p < 0.05$). This statistical significance indicates that the relation between NDVI and soil salinity is caused by one

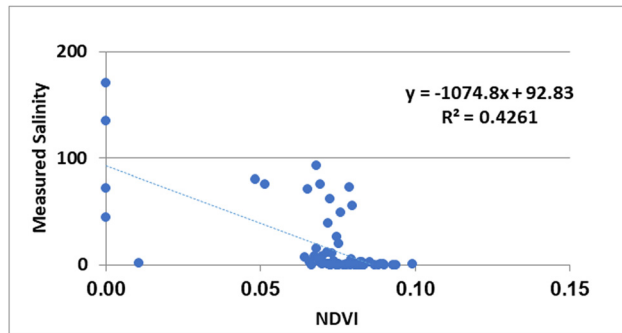


Figure 2: Relation between the measured soil salinity and NDVI.

of them affecting the other and that there is less than 5% probability of rejecting the relation between NDVI and soil salinity. Table 3 and Figure 2 show the regression model quantifying this relation.

$$\text{Salinity} = -1074.8 \times \text{NDVI} + 92.83 \quad (6)$$

NDVI maps of study were produced to explore the seasonal vegetation cover variation and its relation with on soil salinity. The results showed a significant inverse correlation between the NDVI values and soil salinity value ($R^2 = 0.43$). Sabkha soil areas which are located in northern and central regions of the study area have high values of soil salinity and low values of NDVI. On the other hand, the southern region of the study area has the most green-covered area with high values of NDVI and low soil salinity values. Generally, the north-eastern region of the study is lacking the most in terms of vegetation and greenland due to salinization layers which disable plant growth. The salinity of the soil thus plays a larger role in the breakdown of the physical structure of the soil, leading to a loss of the canopy of vegetation in the areas. Therefore, an immediate need is felt to research the causes and consequences of soil salinity.

4.2 The relation between soil salinity and NDVI differs from site to site in the study area

4.2.1 Relation between NDVI and BSI

Figure 3 shows the relation between land degradation (expressed in terms of BSI) and vegetation cover (in terms of the NDVI). Results indicate a statistically significant relation between BSI and NDVI ($p < 0.05$), and the regression model that predicts BSI from NDVI has a moderate

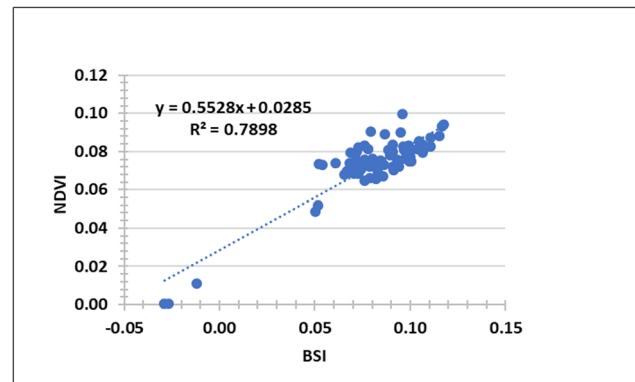


Figure 3: Relation between the NDVI and BSI.

prediction power ($R^2 = 0.79$). This relation is obtained because NDVI and BSI use the red and NIR spectra in the equations. Additionally, BSI reflects the percentage of land degradation when generally considering a low rainfall; however, it does not indicate whether an area is extremely low in vegetation, as estimated by NDVI. Low NDVI values are associated with extreme climatic conditions such as extremely low annual rainfall (≤ 120 mm/year) and high evaporation rates (2,000 mm/year). Furthermore, salinization has negative effects on plant roots, which passively affects plant growth.

The NDVI and BSI maps were produced and compared with each other. The results showed significant positive relationship ($R^2 = 0.79$). The low values of BSI and NDVI were recorded in the north-central regions of the study area, whereas high values were recorded in the southern parts. Despite the presence of saline layers in south-central region, soil moisture in winter contributes to the availability of soil vitality at a minimum level. This means soil salinity plays greater role in preventing the availability of the appropriate environment to increase vegetation cover and soil productivity.

4.2.2 Relation between soil salinity and BSI

We investigated the relation between the measured soil salinity and BSI to determine whether soil salinity leads to land degradation. Results (Figure 4) revealed a statistically significant relation between soil salinity and BSI ($R^2 = 0.25$, $p < 0.05$), indicating a strong evidence against no relation between soil salinity and BSI (Table 3). The relation level was different from the expectations because the salinity in Sabkha soil can be attributed to the salty groundwater near the surface in that area, which is based

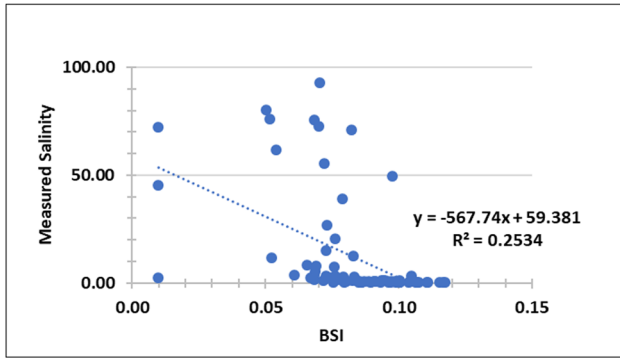


Figure 4: Relation between the measured soil salinity and BSI.

on Al-Mhaidib [64]. Thus, shallow water that can be attributed to droughts or very low rainfall can affect the BSI results. The linear regression model describing the relation between these variables can be expressed as follows:

$$\text{Salinity} = -567.74 \times \text{BSI} + 59.381 \quad (7)$$

BSI maps of the study area are produced to investigate the relationship between the spatial distribution of soil degradation and soil salinity. The BSI values ranged from low to moderate in the northern and central regions of the study area. While the BSI values increase from moderate to high values, the further we move from the shore in south direction and inversely with the soil salinity values, it is therefore very evident that the north-middle direction of the areas is dominated by the humidity and these areas are affected by the impact of salt water, which forms salt layers. Soil moisture from seawater prevents absolute drought and soil degradation in the northern part of the study area, particularly during the winter season, but at the same time contributes to the formation of salinization layers due to the high temperatures caused by hot events during summer season, which affect the reading of RS data in the Sabkha soil area.

Results support that any increase in soil salinity will adversely affect the growth of vegetation, thereby decreasing the NDVI and increasing the BSI. In consideration of these results, the ArcGIS software was used to generate a digital soil salinity map based on the aforementioned regression models using the raster calculator. Regression models were used to estimate and model soil salinity for the study area.

This study aims to present an example of soil salinity mapping based on the soil salinity categories and shows the geospatial distribution of soil salinity within the study area. The soil salinity levels were classified and

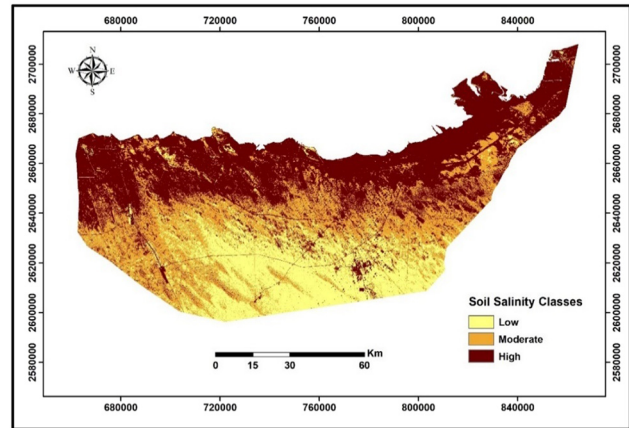


Figure 5: Predicted digital soil salinity map.

mapped based on the classification given by Kissel and Sonon [57]. Figure 5 presents the predicted soil salinity map for the study area generated based on the NDVI-BSI regression model (equation (8)), which can be expressed as follows:

$$\text{Soil salinity} = -284 \times \text{BSI} - 537 \times \text{NDVI} + 76 \quad (8)$$

BSI is sensitive to soil salinity and is thus regarded as a good model for mapping the high soil salinity levels of the Sabkha area. However, this index does not accurately predict low soil salinity levels. This can be attributed to the fact that certain types of soils, such as low salinity soils, show no spectral response in the NIR-SWIR spectral range [9].

The model obtained based on these indices has proved to be capable of mapping and accurately estimating soil salinity at different levels within the study area and has a prediction power of 36% ($R^2 = 0.36$). This model is based on NDVI and BSI, which are calculated using the surface reflectance of NIR radiation, making this a useful tool for monitoring soil salinity.

The study findings show that most saline soils are located in the inland Sabkha, which may be attributed to the salty groundwater near the surface in that area. Al-Mhaidib [64] mentioned that the upward movement of water due to capillary action because of the increased continuous evaporation rate results in increased salinity of Sabkha soils and salt deposition at the top surface of the Sabkha. Additionally, soil salinity is generally higher in the northern part of the study area near the Arabian Gulf, which can be attributed to the deposition of carbonates by wind erosion of inland dunes due to the northerly (Shamal) winds [9]. The nonsaline soils are mostly located in the southern inland parts of the study area.

4.2.3 Relation between soil salinity and LST

The MODIS LST data were analyzed against the *in situ* salinity data. However, some of the daily LST data were excluded from correlation analysis because the corresponding *in situ* salinity data were unavailable. Here, we present the most meaningful and relevant results of the analyses. Results showed no statistically significant relation between LST/NDVI and LST/BSI, with correlations of $R^2 = 0.14$ and 0.05 for LST/BSI and LST/NDVI, respectively. $p < 0.05$ indicates less than 5% probability to reject the relation between LST and various indices, where the effect of LST on vegetation and land degradation is different, as indicated by the correlation values. All the LST data were obtained on November 6, 2016, in correspondence with the *in situ* measurements. Four types of LST data were analyzed against the *in situ* salinity data, and the correlation of all the data varied from 0.22 to 0.56. The nighttime LST data exhibited a significant correlation of greater than 0.4, as shown in Table 4. Results indicate a statistically significant physical process-driven correlation.

The highest positive correlation for salinity can be observed with the nighttime Aqua LST data (0.56; Table 4), whereas the correlation with daytime LST is very low. Figure 6 shows the LST correlation against *in situ* salinity from this highest correlation on November 6, 2016. Thus,

Table 4: LST with salinity *in situ* correlation results

	Aqua_Day	Aqua_Night	Terra_Day	Terra_Night
r	0.22	0.56	0.25	0.43
R^2	0.05	0.32	0.06	0.16

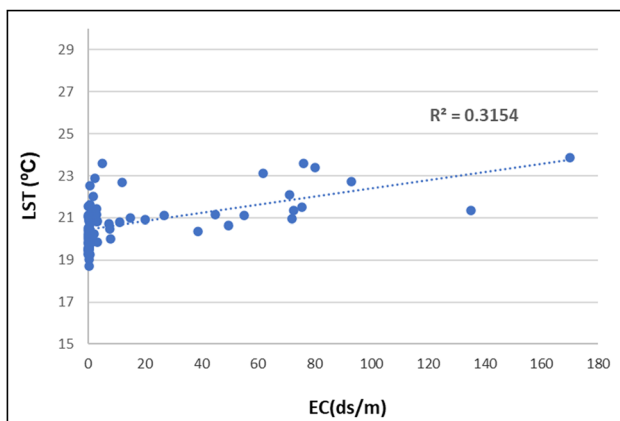


Figure 6: Relation between the nighttime Aqua LST and salinity correlation.

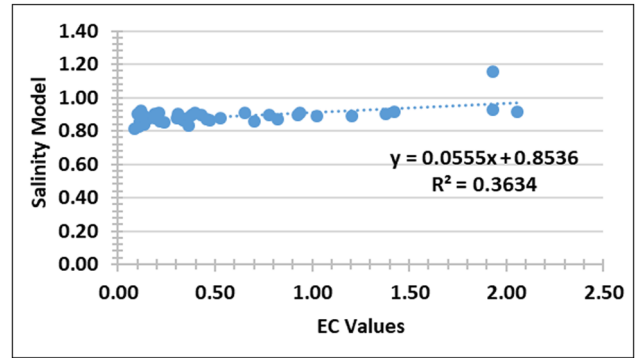


Figure 7: Relation between the measured EC values and soil salinity estimated from the model.

the presented results demonstrate that the best correlation could be achieved using the nighttime LST data. Considering the low spatial resolution of the MODIS data, the obtained results are statistically significant. Results show that salinity will increase more in areas with higher temperatures and that increased temperatures can lead to increased salinity. This assumption is supported by the statistical results, where a correlation of 56% and an R^2 of 0.32 were achieved. For future studies, the number of *in situ* measurements must be increased and satellite data with higher spatial resolution must be used.

4.3 Validation

A low correlation ($R^2 = 0.36$) was found between the measured EC values and the corresponding soil salinity estimates of the model when validating the developed model (Figure 7). Nevertheless, the soil salinity model developed based on NDVI and BSI can be used for detection and prediction in case of salt-affected soils.

Generally, the reflectance in the visible and NIR bands is beneficial for identifying saline and nonsaline surfaces. Many studies [3,5,8,25,62] have shown that spectral indices (e.g., NDVI, SI, SSI1, and BSI) can be used to assess soil salinity and identify the salt-affected areas using imagery data. Thus, the model developed in this study is a promising tool for tracking soil salinity in the study area.

5 Conclusion

We developed a model for estimating and monitoring soil salinity in Abu Dhabi (UAE) using RS-based spectral indices and field measurements of soil salinity. Results support the

possibility of modeling and mapping soil salinity using RS and GIS techniques. The results show that 31% of the soil is moderately salty in the sample region and that 46% of the soil is extremely salty. The findings suggest a statistically significant relationship between NDVI and soil salinity ($R^2 = 0.43$, $p < 0.05$) and a significant relationship between LST/NDVI and LST/BSI, with a correlation between $R^2 = 0.14$ and 0.05 for LST/BSI and LST/NDVI, respectively. The regression model that forecasts NDVI BSI has a medium predictive power ($R^2 = 0.79$). Study findings suggest that any increase in soil salinity will adversely affect vegetation growth. In the light of these findings, the ArcGIS software was used to generate a digital soil salinity map based on the regression models using the raster calculator. The integration of RS data and field measurements is a powerful tool for detecting salt-affected soils. The developed model could detect 77% of the salt-affected soils in the study area. Thus, this model can be confidently used to detect soil salinity in areas experiencing soil salinization. This model's ease of use and acceptable results make it a promising tool for predicting soil salinity. Although the imagery data used in this study are of low resolution ($30\text{ m} \times 30\text{ m}$), the model provides useful results reflecting the variations in soil salinity distribution. Accordingly, this study proves the model's ability to determine degrees of soil salinity in the region using RS data and GIS geospatial analysis for effective soil management and monitoring. In addition, this study showed a low correlation between soil salinity and nighttime LST, indicating that salinity will increase with the increasing temperature. However, the correlation between soil salinity and LST is an ongoing research topic. For future work, we recommend more detailed investigation on this topic by increasing the number of *in situ* measurements and using satellite data with higher spatial resolutions.

Supplementary materials: The imagery data (Landsat 8 OLI (Operational Land Imager), TIRS (Thermal Infrared Sensor)) and MODIS data are available online (<https://earthexplorer.usgs.gov/>).

Acknowledgments: The researchers thank the College of Graduate Studies at United Arab Emirates University for funding this work. The researchers also thank the members of the Department of Earth and Environmental Sciences in Al al-Bayt University for providing all necessary support.

Funding information: This research was funded by the College of Graduate Studies at the United Arab Emirates University.

Author contributions: M. I. and A. A. were involved in conceptualization; M. I. contributed to methodology; M. I., G. K., and A. A. were in charge of software; A. A., A. H., and A. A. were involved in validation; A. A., A. H., and A. A. were in charge of formal analysis; A. A., A. H., and A. A. were in charge of resources; A. A. and A. H. performed data curation; M. I. wrote the original draft; M. I., A. A. and A. A. contributed to writing (review and editing); M. I. supervised the project; A. A. managed the project; A. A. was in charge of funding acquisition. All authors have read, and agreed on, the published version of the manuscript.

Conflict of interest: The authors declare no conflict of interest and that the funders had no role in the design of the study; in the collection, analysis, or interpretation of data; in the writing of the manuscript, or in the decision to publish the results.

References

- [1] Farifteh J, Farshad A, George R. Assessing salt-affected soils using remote sensing, solute modelling, and geophysics. *Geoderma*. 2006;130:191–206.
- [2] Fernandez-Buces N, Siebe C, Cram S, Palacio J. Mapping soil salinity using a combined spectral response index for bare soil and vegetation: a case study in the former lake Texcoco, Mexico. *J Arid Environ*. 2006;65:644–67.
- [3] Ibrahim M. Modeling soil salinity and mapping using spectral remote sensing data in the arid and semi-arid region. *Int J Remote Sens Appl*. 2016;6:76–83.
- [4] Mougnot B, Pouget M, Epema G. Remote sensing of salt affected soils. *Remote Sens Rev*. 1993;7:241–59.
- [5] Wu W, Mhaimeed AS, Al-Shafie WM, Ziadat F, Dhehibi B, Nangia V, et al. Mapping soil salinity changes using remote sensing in Central Iraq. *Geo Reg*. 2014;2:21–31.
- [6] Dehni A, Lounis M. Remote sensing techniques for salt affected soil mapping: application to the Oran region of Algeria. *Proc Eng*. 2012;33:188–98.
- [7] Ibrahim MMF. The use of geoinformatics in investigating the impact of agricultural activities between 1990 and 2010 on land degradation in NE of Jordan. Germany: Verlag Nicht Ermittelbar; 2014.
- [8] Noroozi AA, Homae M, ABBASI F. Integrated application of remote sensing and spatial statistical models to the identification of soil salinity: a case study from Garmsar Plain, Iran. *Environ Sci*. 2011;9(1):59–74.
- [9] Abuelgasim A, Ammad R. Mapping soil salinity in arid and semi-arid regions using Landsat 8 OLI satellite data. *Remote Sens Appl Soc Environ*. 2019;13:415–25.
- [10] Elhag M. Evaluation of different soil salinity mapping using remote sensing techniques in arid ecosystems, Saudi Arabia. *J Sens*. 2016;2016:1–8.
- [11] Al-Khaier F. Soil salinity detection using satellite remote sensing. Enschede, Netherlands: ITC; 2003.

- [12] Zewdu S, Suryabhagavan K, Balakrishnan M. Geo-spatial approach for soil salinity mapping in Sego Irrigation Farm, South Ethiopia. *J Saudi Soc Agric Sci.* 2017;16:16–24.
- [13] Ghassemi F, Jakeman AJ, Nix HA. Salinisation of land and water resources: human causes, extent, management and case studies. Wallingford (United Kingdom): CAB International; 1995.
- [14] Shrestha DP, Farshad A. Mapping salinity hazard: an integrated application of remote sensing and modeling-based techniques. Remote sensing of soil salinization impact on land management. United States of America: Taylor & Francis Group; 2009. p. 257.
- [15] Shrivastava P, Kumar R. Soil salinity: a serious environmental issue and plant growth promoting bacteria as one of the tools for its alleviation. *Saudi J Biol Sci.* 2015;22:123–31.
- [16] Ali R, Moghanm F. Variation of soil properties over the land-forms around Idku lake, Egypt. *Egypt J Remote Sens Space Sci.* 2013;16:91–101.
- [17] El Bastawesy M, Ali RR, Al Harbi K, Faid A. Impact of the geomorphology and soil management on the development of waterlogging in closed drainage basins of Egypt and Saudi Arabia. *Environ Earth Sci.* 2013;68:1271–83.
- [18] El-Bastawesy M, Ali RR. The use of GIS and remote sensing for the assessment of waterlogging in the dryland irrigated catchments of Farafra Oasis in Egypt. *Hydrol Earth Syst Sci Discuss.* 2011;8:10535–63.
- [19] El Bastawesy M, Ali RR, Deocampo DM, Al, Baroudi MS. Detection and assessment of the waterlogging in the dryland drainage basins using remote sensing and GIS techniques. *IEEE J Sel Top Appl Earth Obs Remote Sens.* 2012;5:1564–71.
- [20] Hu J, Peng J, Zhou Y, Xu D, Zhao R, Jiang Q, et al. Quantitative estimation of soil salinity using UAV-borne hyperspectral and satellite multispectral images. *Remote Sens.* 2019;11:736.
- [21] Ibrahim M, Koch B. Assessment and mapping of groundwater vulnerability using SAR concentrations and GIS: a case study in Al-Mafraq, Jordan. *J Water Resour Prot.* 2015;7:588.
- [22] Mehrjardi RT, Mahmoodi S, Taze M, Sahebjalal E. Accuracy assessment of soil salinity map in Yazd-Ardakan Plain, Central Iran, based on Landsat ETM + imagery. *Am Eur J Agric Environ Sci.* 2008;3:708–12.
- [23] Sanaeinejad SH, Astaraei A, Mousavi PM, Ghaemi M. Selection of best band combination for soil salinity studies using ETM satellite images (A case study: Nyshaboer region, Iran). *International conference on geographic information systems;* 2009.
- [24] Lhissou R, El Harti A, Chokmani K. Mapping soil salinity in irrigated land using optical remote sensing data. *Eurasian J Soil Sci.* 2014;3:82.
- [25] Asfaw E, Suryabhagavan K, Argaw M. Soil salinity modeling and mapping using remote sensing and GIS: the case of Wonji sugar cane irrigation farm. *Ethiopia J Saudi Soc Agric Sci.* 2018;17:250–8.
- [26] Garcia L, Eldeiry A, Elhaddad A. Estimating soil salinity using remote sensing data. *Proceedings of the 2005 central plains irrigation conference, Citeseer;* 2005.
- [27] Metternicht G. Analysing the relationship between ground based reflectance and environmental indicators of salinity processes in the Cochabamba valleys (Bolivia). *Int J Ecol Environ Sci.* 1998;24:359–70.
- [28] Metternicht G, Zinck J. Remote sensing of soil salinity: potentials and constraints. *Remote Sens Environ.* 2003;85:1–20.
- [29] Eldeiry AA, Garcia LA. Comparison of ordinary kriging, regression kriging, and cokriging techniques to estimate soil salinity using LANDSAT images. *J Irrig Drain Eng.* 2010;136:355–64.
- [30] Furby S, Caccetta P, Wallace J. Salinity monitoring in Western Australia using remotely sensed and other spatial data. *J Environ Qual.* 2010;39:16–25.
- [31] Hardisky M, Klemas V, Smart M. The influence of soil salinity, growth form, and leaf moisture on the spectral radiance of *Spartina Alterniflora*. 1983;49:77–83.
- [32] Brunner P, Li H, Kinzelbach W, Li W. Generating soil electrical conductivity maps at regional level by integrating measurements on the ground and remote sensing data. *Int J Remote Sens.* 2007;28:3341–61.
- [33] Huete A, Liu H, Batchily K, Van, Leeuwen W. A comparison of vegetation indices over a global set of TM images for EOS-MODIS. *Remote Sens Environ.* 1997;59:440–51.
- [34] Iqbal F. Detection of salt affected soil in rice-wheat area using satellite image. *Afr J Agric Res.* 2011;6:4973–82.
- [35] Steven M, Malthus T, Jaggard F, Andrieu B. Monitoring responses of vegetation to stress. Remote sensing from research to operation. *Proceedings of the 18th annual conference of the remote sensing society United Kingdom;* 1992.
- [36] Zhang T-T, Zeng S-L, Gao Y, Ouyang Z-T, Li B, Fang C-M, et al. Using hyperspectral vegetation indices as a proxy to monitor soil salinity. *Ecol Indic.* 2011;11:1552–62.
- [37] Goossens R, Van Ranst E. The use of remote sensing to map gypsiferous soils in the Ismailia Province (Egypt). *Geoderma.* 1998;87:47–56.
- [38] Fallah Shamsi SR, Zare S, Abtahi SA. Soil salinity characteristics using moderate resolution imaging spectroradiometer (MODIS) images and statistical analysis. *Arch Agron Soil Sci.* 2013;59:471–89.
- [39] Ibrahim M, Abu-Mallouh H. Estimate land surface temperature in relation to land use types and geological formations using spectral remote sensing data in Northeast Jordan. *Open J Geol.* 2018;8:174–85.
- [40] Ibrahim M, Koch B, Data P. Evaluate the effect the land surface temperature in the arid and semi-arid lands using potential remote sensing data and GIS technique. *Int J Glob Warm (Forthcoming articles).* 2020. doi: 10.1504/IJGW.2020.10031655
- [41] Khan NM, Rastoskuev VV, Sato Y, Shiozawa S. Assessment of hydrosaline land degradation by using a simple approach of remote sensing indicators. *Agric Water Manag.* 2005;77:96–109.
- [42] Huete HA. AR a soil-adjusted vegetation index (SAVI). *Remote Sens Environ.* 1988;25:295–309.
- [43] Hu W, Shao MA, Wan L, Si BC. Spatial variability of soil electrical conductivity in a small watershed on the Loess Plateau of China. *Geoderma.* 2014;230:212–20.
- [44] Abou Samra RM, Ali R. The development of an overlay model to predict soil salinity risks by using remote sensing and GIS techniques: a case study in soils around Idku Lake, Egypt. *Environ Monit Assess.* 2018;190:706.
- [45] Ali R, Shalaby A. Response of topsoil features to the seasonal changes of land surface temperature in the arid environment. *Int J Soil Sci.* 2012;7:39.
- [46] Farahat A. Air pollution in the Arabian Peninsula (Saudi Arabia, the United Arab Emirates, Kuwait, Qatar, Bahrain, and Oman):

- causes, effects, and aerosol categorization. *Arab J Geosci.* 2016;9:196.
- [47] Abuelgasim A, Ammad R. Mapping Sabkha Land surfaces in the United Arab Emirates (UAE) using Landsat 8 data, principal component analysis and soil salinity information. *Int J Eng Manuf.* 2017;7:1.
- [48] Lokier SW, Knaf A, Kimiagar S. A quantitative analysis of recent arid coastal sedimentary facies from the Arabian Gulf coastline of Abu Dhabi, United Arab Emirates. *Mar Geol.* 2013;346:141–52.
- [49] Alsharhan A, Kendall CSC. Holocene coastal carbonates and evaporites of the southern Arabian Gulf and their ancient analogues. *Earth-Sci Rev.* 2003;61:191–243.
- [50] Bathurst RG. Carbonate sediments and their diagenesis. Amsterdam: Elsevier; 1972.
- [51] Evans G, Schmidt V, Bush P, Nelson H. Stratigraphy and geologic history of the sabkha, Abu Dhabi, Persian Gulf. *Sedimentology.* 1969;12:145–59.
- [52] Paul P, Tenaiji A, Kulaib A, Braimah N. A review of the water and energy sectors and the use of a nexus approach in Abu Dhabi. *Int J Environ Res Public Health.* 2016;13:364.
- [53] Nachtergaele F. Soil taxonomy—a basic system of soil classification for making and interpreting soil surveys—by Soil Survey Staff, 1999, USDA-NRCS, Agriculture Handbook number 436, Hardbound. *Geoderma.* 2001;3:336–7.
- [54] Shahid S, Abdelfattah M, Arshad K, Muhairbi M, Al Othman Y, Al Haji A, et al. Soil survey for the coastline of Abu Dhabi Emirate. *Reconnaiss Surv.* 2004;1:2.
- [55] Al-Shamsei MH. Drainage Basins and flash flood hazards in Al-Ain area. United Arab Emirates: United Arab Emirates University; 1993.
- [56] Youssef AM, Pradhan B, Sabtan AA, El-Harbi HM. Coupling of remote sensing data aided with field investigations for geological hazards assessment in Jazan area, Kingdom of Saudi Arabia. *Environ Earth Sci.* 2012;65:119–30.
- [57] Kissel DE, Sonon LS. Soil test handbook for Georgia. Georgia: The University of Georgia; 2008.
- [58] Rouse J, Haas R, Schell J, Deering D. Monitoring vegetation systems in the great plains with ERTS. *NASA Spec Publ.* 1974;351:309.
- [59] Carlson TN, Ripley DA. On the relation between NDVI, fractional vegetation cover, and leaf area index. *Remote Sens Environ.* 1997;62:241–52.
- [60] Ibrahim M, Ghanem F, Al-Salameen A, Al-Fawwaz A. The estimation of soil organic matter variation in arid and semi-arid lands using remote sensing data. *Int J Geosci.* 2019;10:576.
- [61] Rikimaru A, Roy PS, Miyatake S. Tropical forest cover density mapping. *Trop Ecol.* 2002;43:39–47.
- [62] Allbed A, Kumar L, Sinha P. Mapping and modelling spatial variation in soil salinity in the Al Hassa Oasis based on remote sensing indicators and regression techniques. *Remote Sens.* 2014;6:1137–57.
- [63] Khan NM, Rastoskuev VV, Shalina EV, Sato Y. Mapping salt-affected soils using remote sensing indicators—a simple approach with the use of GIS IDRISI; 2001.
- [64] Al-Mhaidib Al. Sabkha soil in the Kingdom of Saudi Arabia: characteristics and treatment. *Arts Humanit.* 2003;14:29–82.